Tropospheric distribution of ozone and its precursors over the tropical Indian Ocean

N. Saraf and G. Beig

Indian Institute of Tropical Meteorology, Pune, India

M. Schultz

Max-Planck-Institut für Meteorologie, Hamburg, Germany

[1] To evaluate the atmospheric ozone measurements of the Indian Ocean during the dry winter season from January to March, an analysis of ozone and its precursors has been made using the Model of Ozone and its Related Tracers (MOZART-2), a global chemical transport model. The ozonesonde measurements were made on board the ship *Sagar Kanya* during the Indian Ocean Experiment 1999 (INDOEX-99), which covered the region from 11.3°N to 20.2°S and from 62.3°E to 75.8°E. These measurements reveal surface ozone values on the order of 20–50 ppb over the oceanic region and increasing concentrations in the midtroposphere in the range 50–100 ppb, followed by a steep gradient (>120 ppb) near the tropopause. The model qualitatively reproduces most of the broad features observed in the ozonesonde measurements. The low value of O_3 over the ocean is characterized by the low concentration of NO_x and CO as simulated by the model, but the relationship between O_3 and NO_x breaks down toward the continent where NO_x increases sharply and O_3 does not follow the steep gradient. The variation in CO from ocean to continent is closely related to the O_3 variation. The model reproduces the latitudinal variation of CO in this region well but underestimates the CO concentration by 30–50%, probably because of underestimated emission values. The latitudinal distribution of ozone over the marine boundary layer shows a decrease from north of the equator to the south as the CO-rich air from the continent spreads toward the ocean, thereby reflecting the inflow of pollutants to the pristine marine region during the dry winter season.   *INDEX TERMS:* 0365 Atmospheric Composition and Structure: Troposphere—composition and chemistry; 0368 Atmospheric Composition and Structure: Troposphere—constituent transport and chemistry; 3339 Meteorology and Atmospheric Dynamics: Ocean/atmosphere interactions (0312, 4504); *KEYWORDS:* ozone, troposphere, oceanic region

1. Introduction

[2] Since the advent of the industrial era, increasing human activities have resulted in an enormous growth of pollutants, which are released into the atmosphere. The rising concentrations of trace gases lead to adverse health effects and exert a noticeable influence on the Earth's climate [*Intergovernmental Panel on Climate Change*, 2001]. Tropospheric O_3 plays a vital role in the chemical climate locally and globally. Tropospheric O_3 is a precursor to the OH radical, which ultimately determines the oxidizing capacity of the atmosphere. It is photochemically produced by the photooxidation of pollutants like CO, CH_4, and volatile organic compounds (VOCs) in the presence of NO_x. As the tropical region receives intense solar radiation, photochemical processes are rapid. Several measurements made during NASA's Global Tropospheric Experiment program over the Pacific and Atlantic Oceans have reported distinct pollution plumes of tropospheric ozone and its precursors in the middle and upper troposphere [e.g., *Chameides et al.*, 1989; *Davis et al.*, 1996; *Fishman et al.*, 1996; *Singh et al.*, 1996, 2000; *Schultz et al.*, 1999]. The photochemical destruction of ozone due to this mechanism has been found to be important over the marine boundary layer (MBL) of the central Atlantic Ocean also [*Weller et al.*, 1996]. However, in the middle and upper troposphere of the Pacific and Atlantic Oceans, instances of elevated levels of ozone and its precursors like CO and NO_x have been reported [*Prados et al.*, 1999]. Airborne in situ measurements made during the Pacific Exploratory Mission (PEM) Tropics A (September–October 1996) expedition over the remote South Pacific (10°S–30°S) showed increased levels of ozone from 30 to 90 ppb coincident with CO increase [*Singh et al.*, 2000] in the midtroposphere. These and several other measurements made over the South

Atlantic Ocean again showed that the continental outflow of pollutants due to biomass burning emissions in South America and Africa explains the observed levels of O_3 budget over the tropical South Pacific and the South Atlantic basin [*Fishman et al.*, 1996; *Schultz et al.*, 1999; *Chatfield et al.*, 2002; *Staudt et al.*, 2002]. In contrast, during the West A part of the PEM airborne expedition carried out in September–October 1991 over the equatorial and tropical Pacific, low ozone values (8–9 ppb) in the MBL were reported [*Singh et al.*, 1996]. Such low values of ozone in the MBL were attributed to weak downward mixing from the free troposphere and the in situ photochemical destruction via the reactions $O_3 + h\nu \rightarrow O_2 + O(^1D)$, $O(^1D) + H_2O \rightarrow 2OH$, and $O_3 + HO_2 \rightarrow OH + 2O_2$. Measurements made over the convective regions of the equatorial Pacific in March 1993 have shown low O_3 concentrations on the order of 10 ppb in the MBL, around 10 km, and at the tropopause [*Kley et al.*, 1996].

[3] The Indian Ocean is bounded by continental landmasses to the west (Africa) and to the north (the Indian subcontinent). The eastern boundary is marked by the Malaysian peninsula and the Indonesian islands. Significant pollutant emissions occur on all of these landmasses at different times of year. Vegetation fires in Africa are burning almost year-round, with peak intensities during December–January north of the equator and September–November in the Southern Hemisphere. Indian emissions consist largely of domestic fuel wood burning, but the fossil fuel source has also increased significantly over the past decades. Indonesia also has significant fossil fuel emissions and an intensive burning season in spring. During the Northern Hemisphere winter, when the winds are northeasterly over the Indian region, the polluted continental air mixes with the pristine marine air from the Southern Hemisphere through the intertropical convergence zone (ITCZ). The warm waters of the Indian Ocean trigger a deep convective cloud system, which, in association with the ITCZ, results in the vertical mixing of trace gases like O_3, NO_x, CO, and nonmethane hydrocarbons (NMHCs) [*Kley et al.*, 1996; *de Laat et al.*, 1999]. Using a three-dimensional (3-D) chemistry transport model, *de Laat et al.* [1999] have simulated O_3 profiles characterized by low surface O_3, midtropospheric maxima, and upper tropospheric minima over the Indian Ocean during spring 1995. The low values of the upper tropospheric minima were attributed to the convective transport of O_3-depleted boundary layer air in the ITCZ [*de Laat et al.*, 1999]. Midtropospheric maxima and laminae of O_3 found in several cases with concentrations peaking up to 120 ppb have been reported by *Zachariasse et al.* [2000], who link them to the stratosphere-troposphere exchange (STE) process.

[4] The Indian Ocean is one of the least explored ocean regions so far. Therefore a major research effort was initiated to understand the environment over the Indian Ocean. The Indian Ocean Experiment (INDOEX) measured the extent of aerosols and trace gas species like ozone and some of its precursors during the period 1996–1999. The research vessel R/V *Malcolm Baldrige* of the U.S. National Oceanic and Atmospheric Administration measured several chemical species during March and April 1995. Similar measurements were made on board the Indian ship R/V *Sagar Kanya* as part of the INDOEX program during the years 1996–1999.

Some modeling studies have been carried out to understand the chemical climate over the Indian Ocean during the pre-INDOEX cruise of 1995 [*Rhoads et al.*, 1997; *Dickerson et al.*, 1999]. To properly understand these experimental results related to ozone over the Indian Ocean as measured during the *Sagar Kanya* INDOEX-99 cruise, we have used a state-of-the-art chemistry transport model (CTM) with assimilated meteorological data.

[5] The aim of this paper is to evaluate the tropospheric ozone measurements of the INDOEX period from January to March 1999 during the dry winter season. Ozone measurements made during the *Sagar Kanya* cruise path, which covered the region from 11.3°N to 20.2°S and from 62.3°E to 75.8°E are presented. These measurements are compared with the modeled distributions obtained using a 3-D chemical transport model to characterize the atmospheric chemical composition of its precursors, namely, NO_x and CO, over the INDOEX region and to explain some of the unsolved questions.

2. Model Description

[6] To study the distribution of ozone and its precursors over the Indian Ocean region during the months of January–March, we have used the global CTM, the Model of Ozone and its Related Tracers (MOZART-2) [*Horowitz et al.*, 2003], which is a recent update to MOZART-1 [*Brasseur et al.*, 1998; *Hauglustaine et al.*, 1998]. The MOZART-2 is run with assimilated meteorological data from the European Centre for Medium-Range Weather Forecasts (ECMWF) with a standard resolution of $\sim1.8°$ in longitude and latitude and 31 vertical levels from the surface to 10 hPa. The model considers surface emissions of several chemical compounds (N_2O, CH_4, NMHCs, CO, NO_x, CH_2O, and acetone). The model accounts for the distribution of 63 chemical species reacting in 168 reactions, including 33 photolysis reactions. The emissions due to fossil fuel combustion, agricultural burning, and biofuel use follow the distribution of the Emission Database for Global Atmospheric Research (EDGAR) version 2.0 inventory [*Olivier et al.*, 1996] with seasonality from the Intermediate Model for Annual and Global Evolution of Species (IMAGES) [*Müller*, 1992]. The spatial and temporal distributions of savanna are taken from *Hao and Liu* [1994], and the spatial and temporal distributions of forest fires are taken from *Müller* [1992]. At the time the simulations were performed, the most recently available emissions estimates from EDGAR indicated a substantial overestimate of agricultural waste burning and a significant underestimate of biofuel use emissions of CO, in particular for the Indian subcontinent (C. Granier, personal communication, 2001). In order to reflect these developments the CO emissions were scaled with a globally uniform factor of 0.077 for agricultural waste burning and 1.36 for biofuel use. The resulting emissions for India are 5.2 Tg CO/yr from fossil fuel combustion, 51.9 Tg CO/yr from biofuel use, and 3.6 Tg CO/yr from agricultural waste burning. In comparison, the most recent estimates from EDGAR 3.2 [*Olivier and Berdowski*, 2001] list 1995 emissions of 4.0, 48.6, and 1.0 Tg CO/yr, from fossil fuel combustion, biofuel use, and agricultural waste burning, respectively. Forest and savanna fires
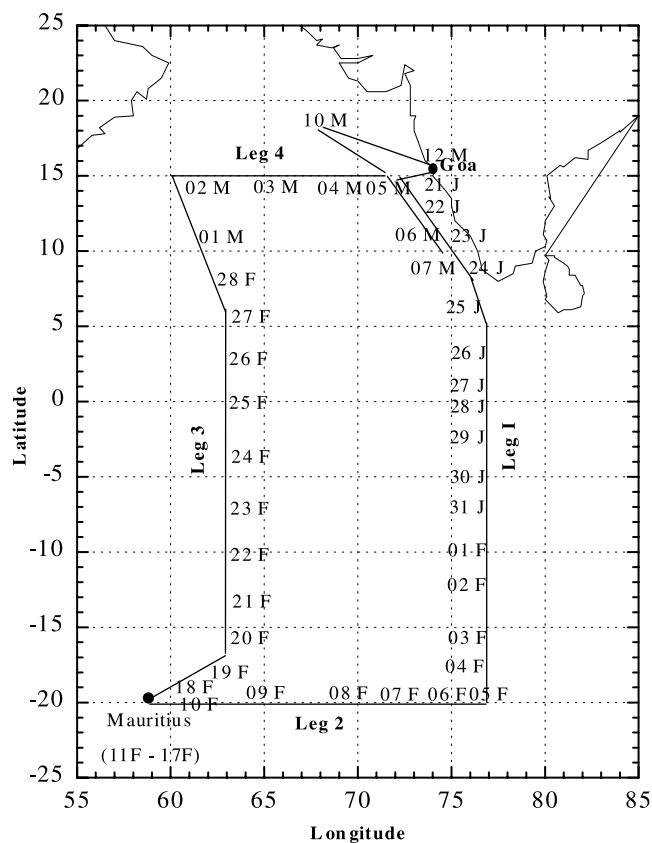
Figure 1. Cruise path of the *Sagar Kanya* during the Indian Ocean Experiment Intensive Field Phase (INDOEX-IFP) in 1999. The four different legs, namely, legs 1–4, identified to evaluate the results in this work are marked clearly.

contribute another 6 Tg CO/yr to the emissions from the Indian subcontinent in the MOZART-2 inventory.

3. Ozonesonde Data

[7] The ozonesonde measurements discussed here were made with modified electrochemical Brewer-Mast bubbler ozone sensors with nonreactive Teflon pumps [*Sreedharan*, 1968]. The sensors consist of an electrolyte cell containing a solution of buffered potassium iodine through which ambient air is sucked by a small pump. The quality of the electrochemical concentration cell (ECC) and the Indian ozonesonde was assessed in several intercomparisons [*World Meteorological Organization*, 1994; *Smit et al.*, 1996]. The Jülich Ozonesonde Intercomparison Experiment 1996 (JOSIE) addressed the key shortcomings of earlier intercomparisons. The result of the JOSIE intercomparison showed that the relative deviation of the Indian ozonesonde is typically within ±10–20%, whereas it was within ±10% with respect to the ECC ozonesonde in the third World Meteorological Organization intercomparisons in 1991. The precision error is about ±10–15%. However, the relative precision in the middle stratosphere, where maximum ozone is available, is the best. A normalization factor has been used to check the quality of the data. During INDOEX 1998 and 1999 an intercomparison of ECC and Indian ozonesonde was made, and a coherent pattern was observed at all the altitudes [*Peshin et al.*, 2001]. A total of 39 balloon-

borne ozonesondes was launched from the ship *Sagar Kanya* during the intensive field phase of INDOEX from January to March 1999. These measurements were distributed over the latitudes 11.3°N to 20.2°S and over the longitudes 62.3°E to 75.8°E during the southbound journey of the cruise and over the latitudes 16.9°S to 17.1°N and longitudes 62.3°E to 68.6°E during leg 3. The ship was docked at Mauritius during 9–19 February.

[8] The cruise path of the *Sagar Kanya* for INDOEX-99 is shown in Figure 1. The cruise consisted of four legs: leg 1, 11.3°N to 20.2°S, with longitude fixed ∼75.8°E (21 January to 5 February); leg 2, 75.8°E to 62.3°E, with latitude fixed ∼20.2°S (5 February to 9 February); leg 3, 20.2°S to 15°N, with longitude fixed ∼62.3°E (19 February to 2 March); and leg 4, 60.6°E to 68.6°E, with latitude fixed ∼15°N (2 March to 12 March).

4. Results and Discussion

[9] Figures 2 and 3 show the tropospheric distribution of ozone over the INDOEX cruise path (Figure 1) as obtained by ozonesonde measurements and the MOZART model for legs 1 and 3, respectively. The model results of tropospheric ozone are derived along the ship cruise track and are compared with observations for particular dates. The main features are values of ozone of the order of 10–20 ppb over the ocean surface, with higher values in the midtroposphere (30–70 ppb) and a sudden increase up to 80–100 ppb near the tropopause. The plots clearly show the decreasing gradient observed in the values of ozone as the ship moves from the coast (11.3°N, 74.5°E) to the ocean (20°S, 62.3°E).

[10] The surface values of ozone near the Indian subcontinent on 21 January 1999 are about 50–70 ppb. The concentrations decrease toward the ocean (Figure 2). We have also compared the model-simulated ozone values with those observed by *Dulichand et al.* [2001] along the same cruise path in order to assess the performance of the model, especially at the surface (not shown in Figure 2). The ozone volume-mixing ratio over the latitudinal range extending from 5°S to 20°S varies from 5 to 20 ppb when the ship moves toward the deep marine region. The model simulates the observed values very well within the ±10 ppb range over the oceanic region during leg 1 of the cruise. Discrepancies between the observed and the model-simulated values are found near the continental region, especially between the model-simulated and the ozonesonde-observed surface values. The model gives slightly higher ozone values as compared to the observed values during leg 1 of the cruise.

[11] During leg 3 of the cruise (Figure 3) the model simulates slightly lower surface ozone values along the entire cruise track as compared to the values observed by *Dulichand et al.* [2001]. However, the general trend of increasing surface ozone values toward the continent is seen in the modeled as well as the observed mixing ratios. Along the latitude range 10°N–20°N the values of surface ozone during leg 3 of the cruise are lower (∼30–50 ppb) than during leg 1 (50–70 ppb) along the same latitudes. During leg 3 the ship's track lies mostly over the oceanic region far away from the influence of the continent (Figure 1).

[12] A striking difference between the model and the observed values was seen on 2 February (14.97°S, 77.0°E). The observed vertical ozone profile showed unex-
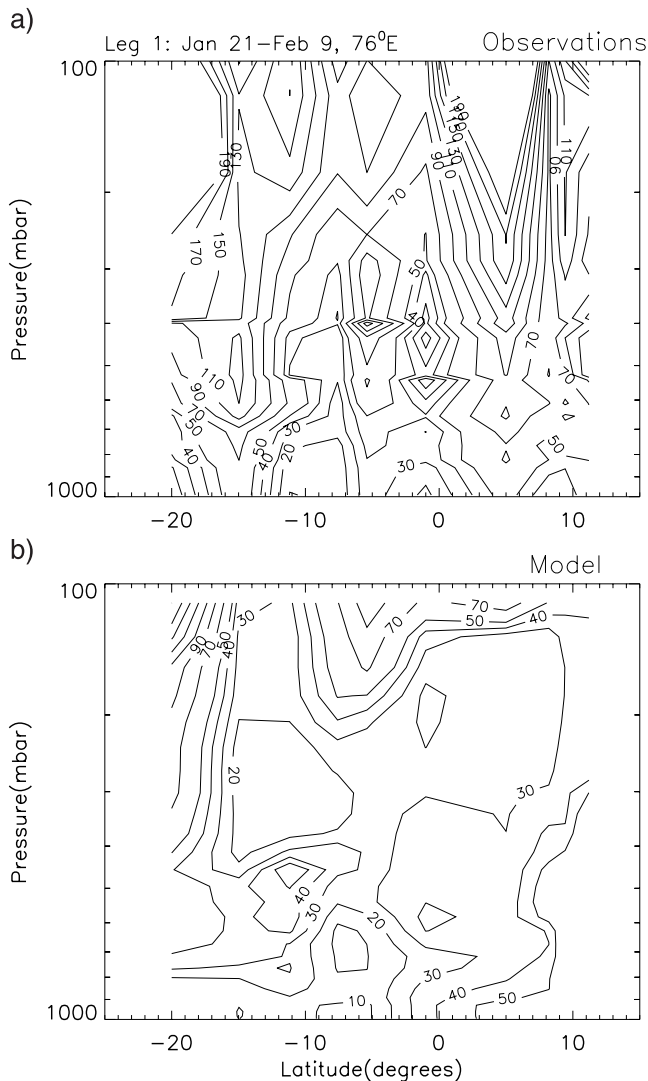
a)

b)

Figure 2. Contour plots of tropospheric ozone distribution along leg 1 cruise path of INDOEX-99 as obtained by (a) ozonesonde observations and (b) model simulations.

pectedly high concentrations of 50–130 ppb everywhere below 600 hPa (not shown in Figure 3). These values are about a factor of 2 higher than those of any other profile measured in the Southern Hemisphere during the cruise, and the model does not reproduce them. While similar upper boundary layer and free tropospheric concentrations are occasionally observed during the Northern Hemisphere transects, the data from 2 February do not exhibit the typical gradient of decreasing concentrations close to the surface. The ECMWF wind fields indicate advection from the south and southeast, from where relatively clean air should be advected. We have found no indication of exceptional emissions from biomass burning or lightning upwind of the study region. The surface observations from *Dulichand et al.* [2001] do not show such high surface values, and the model compares very favorably with these data (S. Lal, personal communication, 2002). Therefore it appears likely that the ozonesonde observations are incorrect for 2 February; hence these particular data points are discarded in this analysis and are not shown in Figure 2.

[13] The comparatively low surface values over the ocean can be explained on the basis of photochemical destruction that takes place in the low-NO_x environment via reactions $O_3 + h\nu \rightarrow O_2 + O(^1D)$ and $O(^1D) + H_2O \rightarrow 2OH$. The model simulates a net photochemical ozone destruction rate of about 2–6 ppb/d over the oceanic region. Hence the observed ozone values over the marine region may be a result of the dynamical influence from the stratosphere and also the continental air being transported to the ocean. The stratospheric contribution to the surface ozone values over the ocean as obtained from the model is about 0–20 ppb, which agrees well with the observed concentrations on several occasions.

[14] It has been speculated that reactions of ozone with biogenic halogens could constitute another major loss process for ozone in the MBL [*Vogt et al.*, 1996; *Dickerson et al.*, 1999; *McFiggans et al.*, 2000]. However, low concentrations of CH_3I found during the PEM-West A airborne expedition over the Pacific Ocean have eliminated iodine chemistry as playing a dominant role in the loss of ozone, especially in the tropics [*Singh et al.*, 1996]. These
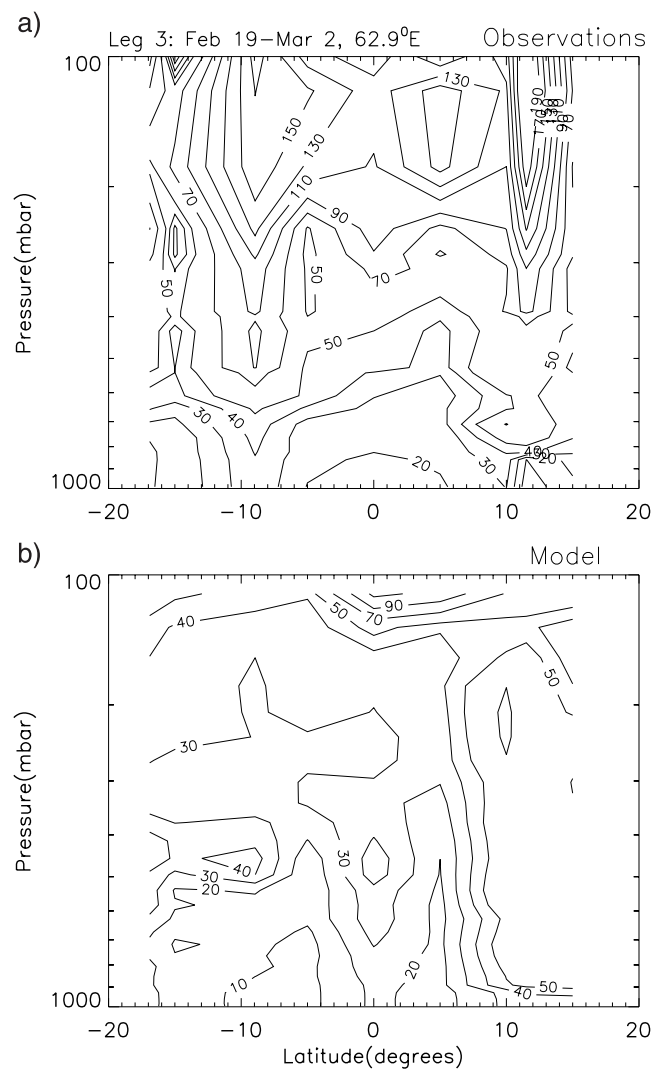
a)

b)

Figure 3. Contour plots of tropospheric ozone distribution along leg 3 cruise path of INDOEX-99 as obtained by (a) ozonesonde observations and (b) model simulations.
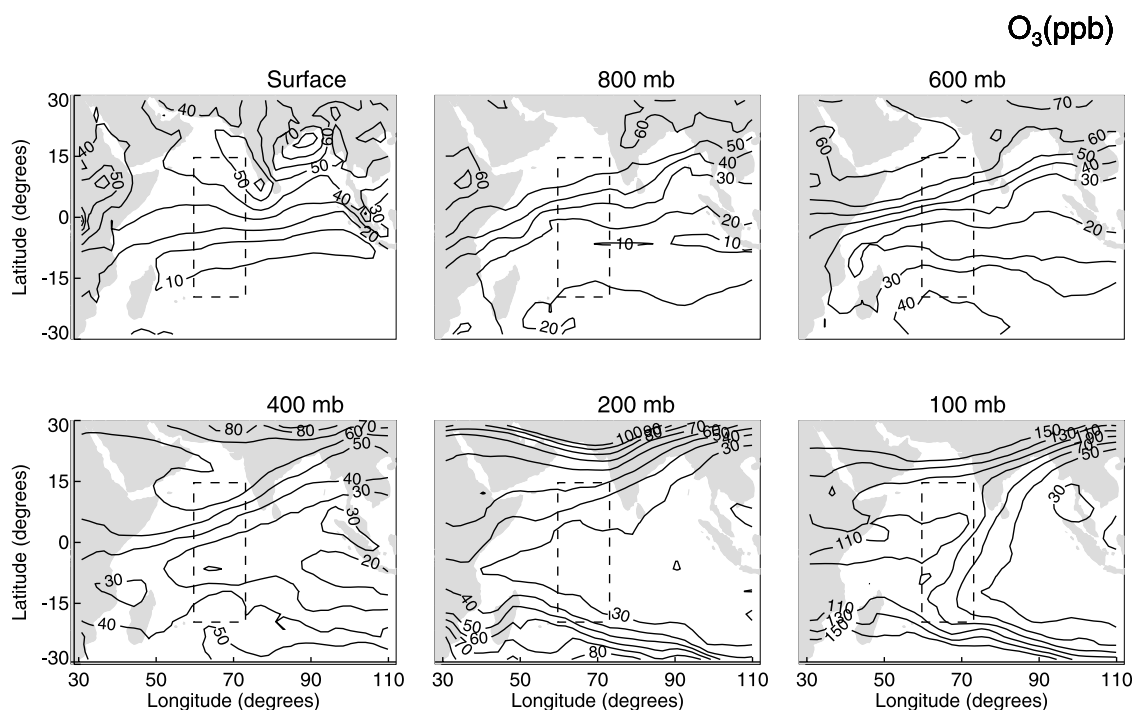
O_3(ppb)

Figure 4. Geographical distribution of ozone (ppb) over the latitude (30°S, 30°N) and longitude (30°E, 110°E) plane covering the Indian Ocean and a part of the Indian subcontinent averaged during the period 21 January to 10 February as obtained in the present model study. Figure 4 shows six plots for different heights: 0, 1, 4, 7, 12, and 16 km.

reactions are not included in the chemical mechanism of our model, so we cannot test their importance for the conditions of the INDOEX cruise. The fact that the model tends to underestimate ozone in the MBL would argue against a significant impact of halogen chemistry under these conditions. However, comparison with CO measurements from the *Sagar Kanya* (see discussion below) indicates that precursor emissions in India may be underestimated by about a factor of 2 in the model. Together with the uncertainties in the ozone deposition flux, we cannot exclude the possibility that halogens could be significant for the marine boundary layer ozone budget.

[15] In the midtroposphere the observed values reach 50–110 ppb and then increase sharply to values >120 ppb just near the tropopause. There are instances when still higher (>150 ppb) concentrations of ozone are found near the tropopause. In the free troposphere the model values are of the order of 20–70 ppb. The higher ozone values in the midtroposphere can be explained well by the photochemistry of ozone and its precursors. The model simulates high values of NO_x in the midtroposphere of $\sim$10–100 ppt (Figures 7b and 8b). The lifetime of NO_x increases with altitude in the troposphere. In the midtroposphere (>8 km) over the tropics, $O_3 + HO_2$ also acts as the single largest O_3 loss process in conjunction with the reaction $O^1(D) + H_2O$ [*Davis et al.*, 1996]. As the concentration of the hydroxyl radicals decreases with increasing altitudes, the photochemical production of O_3 in the presence of NO_x is more favored, thereby resulting in a net production of ozone. The model gives a net production rate of the order of 0–2 ppb/day in most of the midtroposphere. The model-derived ozone concentrations at the pressure levels 800–500 hPa are lower than the observed ones during most of the period. This might

be due to low NO_x values simulated in the midtroposphere. The calculated low value of NO_x is probably a result of either the low stratospheric input, an underestimate of the lightning NO_x production, or too little NO_x being brought up from the boundary layer in the convection. This aspect will need to be further investigated in the model. Recent work by *Lelieveld et al.* [2001] has shown that biomass burning and fossil fuel burning during the winter monsoon in the Indian subcontinent are the main cause of widespread pollution over the Indian Ocean, especially in the midtroposphere. Back trajectory analyses over the INDOEX period have also shown that the air masses originating from the Indian subcontinent, south and Southeast Asia, and Africa are reaching the otherwise clean environment of the Indian Ocean [*Peshin et al.*, 2001]. The lower values of the midtropospheric ozone concentrations may be due to the underrepresentation of biomass burning sources of VOCs and CO. Ozone concentrations almost equal to surface values are also seen in the midtroposphere, which may be due to the deep convection associated with the ITCZ. The deep convective cells of the ITCZ may carry the surface ozone values ($\sim$30–50 ppb) to midtropospheric heights ($\sim$400 hPa). In the upper troposphere, chemical ozone formation is facilitated by the low humidity, cold temperatures, and relatively high NO_x concentrations of $\sim$200 ppt. Nevertheless, near-zero ozone concentrations in the middle and upper troposphere have been observed earlier in the convective regions of the Pacific Ocean by *Kley et al.* [1996], who attribute them to convection lifting the O_3-poor MBL air to the upper troposphere in the Pacific Ocean.

[16] The model-simulated values (80–150 ppb, not shown in Figures 2b and 3b) of ozone just below the tropopause and in the upper troposphere are slightly lower
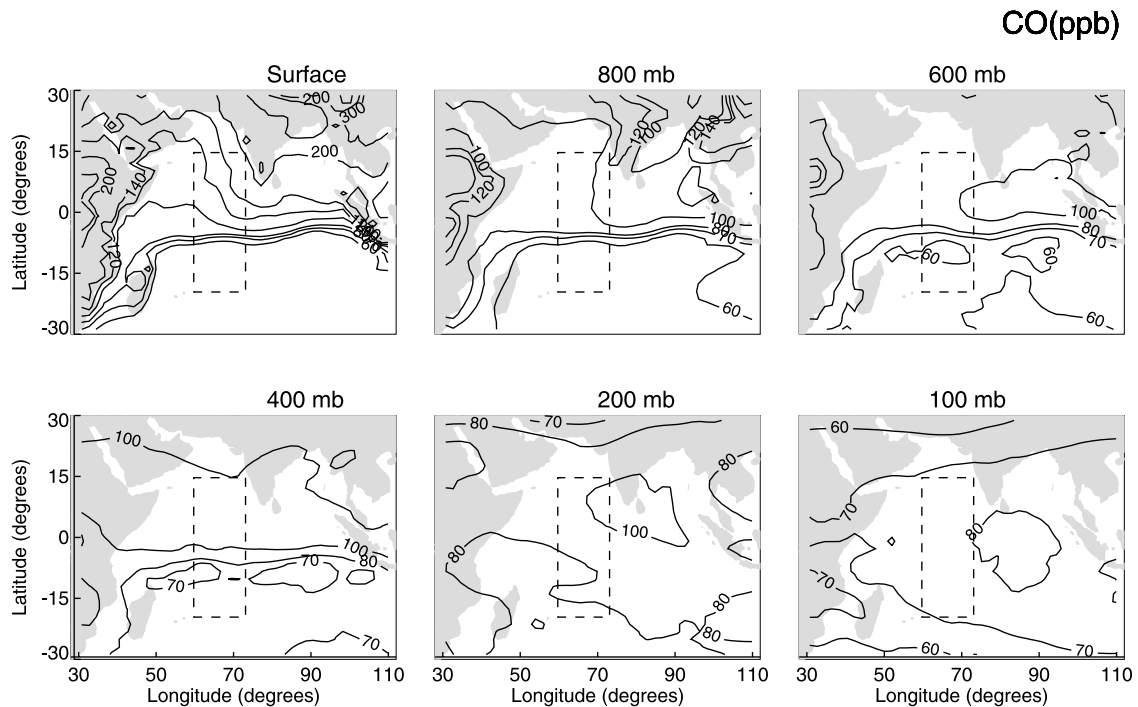
Figure 5. Same as Figure 4 but for CO (ppb).

than the observed values (120–190 ppb), even though the STE flux simulated in the present MOZART-2 runs with ECMWF winds is ~800 Tg/yr, which is significantly higher than the estimates by *Murphy and Fahey* [1994] and *Holton et al.* [1995]. Apparently, the model systematically underestimates the cross-tropopause flux in the vicinity of the subtropical jet. In some cases the structure of the stratospheric ozone tracer in the model compares very well with the ozonesonde observations in the upper troposphere, although the absolute values are low by a factor of 2 (~60 ppb). Agreement would be good if the simulated tropospheric concentration were higher by a factor of 2 and were more or less constant throughout the free troposphere. Further analyses also suggest that the simulations might miss some pollution influences, e.g., from vegetation fires in Africa, which are concentrated in the Northern Hemisphere during this season. The pollution plumes observed over this region also show a stratospheric intrusion event. The very high values near the upper troposphere have been studied by some of the earlier researchers [e.g., *de Laat et al.*, 1999; *Zachariasse et al.*, 2000]. Most of them have attributed these high values to the downward stratospheric influx of O_3 due to the subtropical jet stream (STJ), which occurs near the latitude belts of 30°N and 30°S, though the contribution of STE to the upper tropospheric O_3 maxima in the low latitudes is still not clear [*Roelofs and Lelieveld*, 1997] and needs further study.

[17] The model-simulated geographical distributions of O_3, CO, and NO_x volume-mixing ratios have been plotted in Figures 4, 5, and 6, respectively, for the region from 30°E to 110°E and from 30°S to 30°N. The values plotted are averaged over the period from 21 January to 10 February, which coincides with the outward journey of the INDOEX-99 cruise. These plots are made for different heights (surface, 1, 4, 7, 12, and 16 km) and pressures (800, 600, 400, 200, and 100 mb) as indicated in Figures 4–6. The ozone plots (Figure 4) clearly show the existence of moderate O_3 values (~10–20 ppb) over the entire Indian Ocean south of the equator at the surface and at 1 km. Ozone starts to increase north of the equator toward the Indian subcontinent. The concentration reaches ~50 ppb over south India. The very low value of NO_x (of the order of 2 ppt) found over the ocean, as indicated in Figure 6 at the surface and at 1 km altitude, clearly shows a pollution-free environment south of the equator.

[18] Similarly, the CO distribution (Figure 5) at the surface depicts values in the range of 60–100 ppb over the ocean, which increase to values as high as 140–200 ppb near the coastal region. We have compared the surface CO values as observed by *Dulichand et al.* [2001] with the model-simulated values in the present work. The general trend of decreasing CO values toward the oceanic region is seen in both the observed and the modeled mixing ratios, but the absolute values disagree by 30–50%, with the model being low. The observed CO values lie in the range 50–300 ppb along the entire *Sagar Kanya* cruise track, whereas the model surface CO concentrations are of the order of 50–250 ppb along leg 1 and as low as 100 ppb along leg 3. This indicates that the emissions from the Indian subcontinent are severely underestimated in the model. The geographical distributions (Figure 5) do not show much longitudinal gradient in the concentration of CO at all altitudes. *Stehr et al.* [2002] also measured surface ozone and CO during the INDOEX-99 period from 22 February to April 1 on board the ship R/V *Ronald H. Brown*. We could not make a one-to-one comparison with their data since the time period and cruise track of observation differed from that of the *Sagar Kanya*. However, the average concentrations of CO found from their analysis also show values of the order
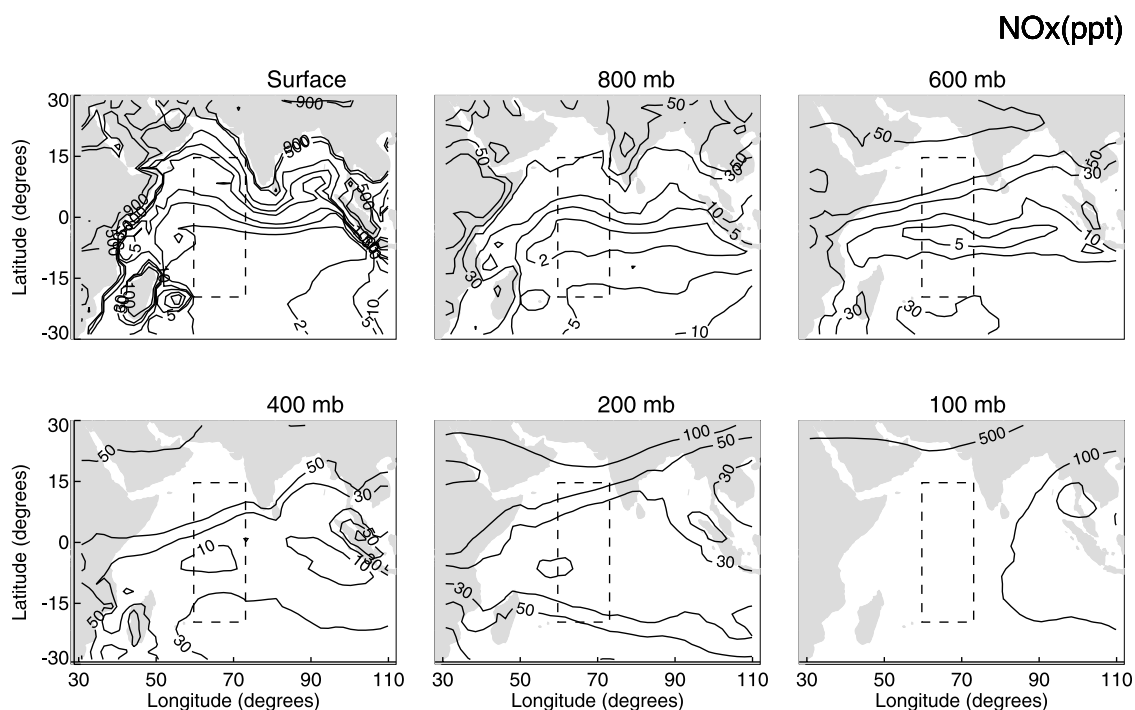
NOx(ppt)

Figure 6. Same as Figure 4 but for NO_x (ppt).

of 50−225 ppb over the entire cruise track (for details, refer to *Stehr et al.* [2002]).

[19] As can be seen from Figures 4−6, the extent of the transport of CO latitudinally from the coastal region to the ocean is larger than that for NO_x and O_3. This is mainly due to the lifetime of CO ($\sim$2−3 months), which is much longer than that of O_3 or NO_x. However, once O_3 or NO_x is lifted up from the planetary boundary layer into the free troposphere, its lifetime increases, making the transport of these species to distant regions possible. It has been shown that the effect of the transport of pollutants from the Indian subcontinent to the Indian Ocean is greater than that from the Southeast Asian region or from the African continent [*Peshin et al.*, 2001]. In the Indian subcontinent, winter (December, January, and February) is the dry season, during which biomass and biofuel burning are high. (The model does not exhibit a seasonal variation for biofuel burning.) As the tropics are a region of intense convective activity, the pollutants get transported to the open marine region and consequently affect the ozone budget there by the usual photochemical production of ozone [*Baldy et al.*, 1996]. The ozone and NO_x values, just below the tropopause near the latitudes 30°N and 30°S increase dramatically to the order of 80−150 ppb and 200−300 ppt, respectively. If such high values are due to the continental transport of pollutants at these heights ($\sim$200−100 hPa), then there should be a similar gradient in the value of CO as well. However, it is seen that the CO values near the tropopause and just below it ($\sim$12 km) show a divergence from the equator toward the latitudes 30°N and 30°S, which is an indication of the outflow of the pollutants from the ITCZ at upper tropospheric heights. Such high values of ozone near the latitudes 30°N and 30°S may be an indication of the stratospheric influence of ozone that takes place near the STJ stream at these latitudes. It has also been shown earlier that

the air near this tropospheric region has a low level of relative humidity ($\sim$10%) [*Peshin et al.*, 2001], which is an indication that the air mass is of stratospheric origin.

[20] To further illustrate the ozone distributions, the meridional cross sections of the vertical distributions of CO and NO_x from MOZART for legs 1 and 3 are plotted in Figures 7 and 8, respectively. The extent of high CO concentrations can be seen as far as the equator in the months during the cruise period. Because of the longer lifetime of CO (2−3 months), the CO emissions from biomass and fossil fuel burning in Africa and India spread latitudinally up to the ITCZ region, which lies in the latitudinal belt 0°S−15°S during this period of the year. However, as the height above the boundary layer increases, the CO concentrations decrease and become as low as $\sim$70−90 ppb in the upper troposphere. A latitudinal gradient from north to south in the surface values of NO_x is also simulated during the entire period, as shown in Figures 7b and 8b. Over the ocean the values drop down to $\sim$2 ppt for the latitude range $\sim$5°S−18°S. In such a low-NO_x environment the O_3 concentration (Figure 2) is found to be $\sim$10−20 ppb. The NO_x values are found to be very high, around 500 ppt, near the continent at 10°N−20°N during January and February along the longitude 76°E. However, NO_x drops down to as low as $\sim$5−10 ppt in February−March (longitude fixed to 62°E) over the latitude range 10°N−20°N. The NO_x lifetime in the planetary boundary layer is on the order of a few days or less [*Hauglustaine et al.*, 1998]. Hence the spread of NO_x from the continent to the ocean is limited by its short lifetime. The low values of NO_x of the order of 10−20 ppt as obtained from the model along legs 1 and 3 of the cruise may be another reason for the discrepancy obtained between the observed and simulated ozone concentrations. The discrepancy is reduced on several occasions during the months of February and March (along
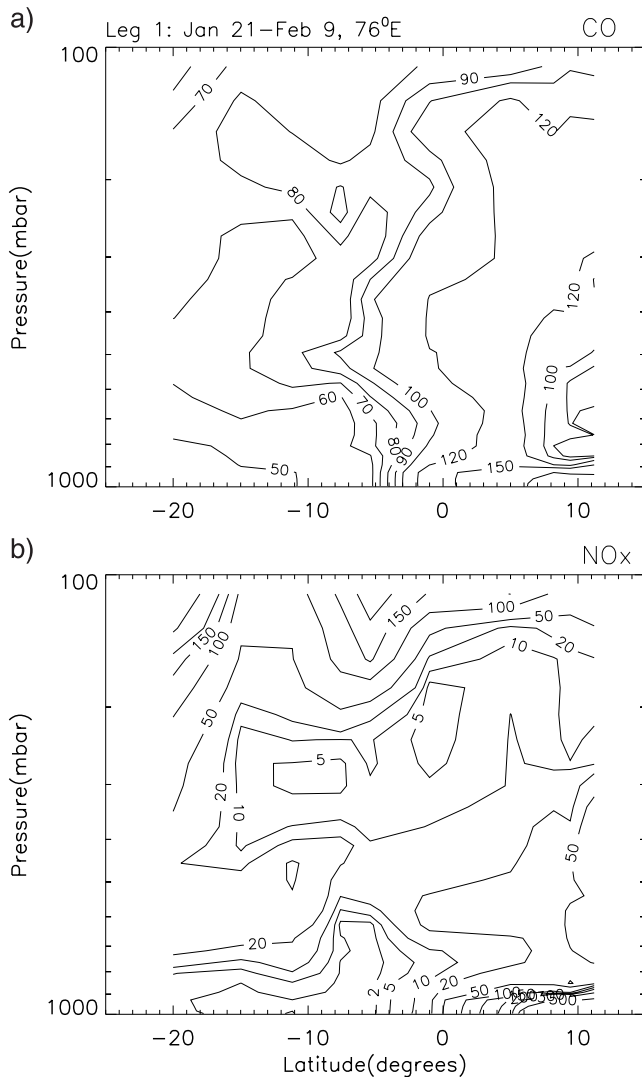
a)

b)

The characteristics of the measured distribution of ozone are examined, and an attempt has been made to interpret them using the global CTM MOZART-2. The observed ozone over the Indian Ocean is marked by moderate values (20–50 ppb) followed by an increasing trend in the mid-troposphere (50–100 ppb) and a steep gradient near the tropopause (>120 ppb). However, near the equatorial belt, deep convective processes over the oceanic surface tend to lift the surface ozone concentrations to midtropospheric heights, which is well simulated by the model. Near the upper troposphere, STE is suggested to be acting as a contributing factor in elevating the ozone concentrations to values >120 ppb. However, the model-simulated values do not show such high levels of ozone concentrations near the upper troposphere and the tropopause in spite of the fact that the Hamburg MOZART-2 runs with ECMWF winds simulate a rather high STE flux on the order of 800 Tg/yr. The variation of ozone and its precursors with longitude is found to be minimal, but the latitudinal variation is highly noticeable. The value of NO_x is found to vary greatly from the ocean (~2 ppt) toward the continent (~500 ppt at the

a)

b)

Figure 7. Model-simulated tropospheric vertical distribution of (a) CO (ppb) and (b) NO_x (ppt) along the latitudinal range 20°S–20°N. The values are obtained along the cruise track for the period 21 January to 9 February along the longitude 76°E (leg 1).

fixed latitudes) when the upper tropospheric NO_x values as obtained by the model have a range in the order of 50–200 ppt. The strong anticyclonic conditions that were prevalent in the Arabian Sea during the months of January and February brought more pollutants to the Indian Ocean than during February and March [*Dulichand et al.*, 2001]. This is very well represented in the simulated values of surface O_3, CO, and NO_x as well in the observed values of surface ozone. The rate of decrease in the observed ozone concentration along the two longitudes and same latitude ranges (10°N–20°N) does not occur at the same rate as the NO_x decrease, thereby depicting the nonlinear relationship between ozone and NO_x.

5. Conclusions

[21]   The tropospheric distributions of ozone and its precursors, namely NO_x and CO, over the Indian Ocean region for the period from January to March 1999 are presented.
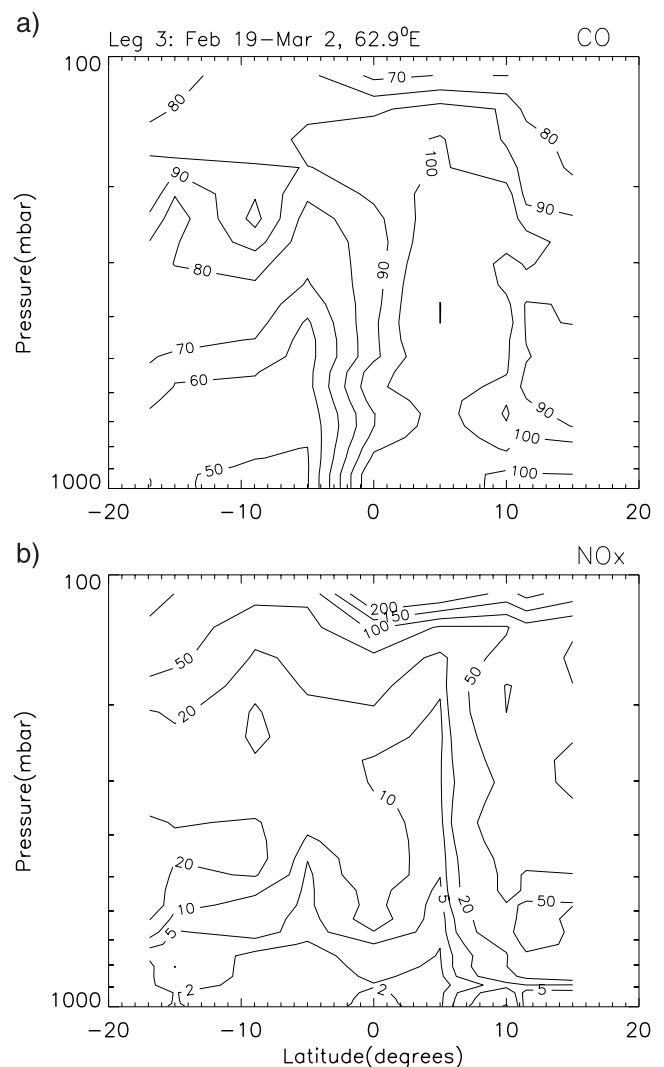
Figure 8. Same as Figure 7 but for fixed longitude 62.9°E and the values obtained for the period from 19 February to 2 March (leg 3).

grid point 20°N, 76°E). The ozone concentrations do not follow the linear NO_x enhancement pattern when the results along the longitude 76°E are compared with results along the longitude 62°E. It is found that the distribution of ozone is better correlated with CO than with NO_x. The role of bromine and iodine catalytic reactions on the sea salt aerosol surfaces in explaining the low concentrations of ozone over the marine region cannot be substantiated in this study, but it cannot be excluded either. These processes need to be studied further in detail in order to successfully understand and explain the chemistry of ozone over the tropical Indian Ocean.

References

Baldy, S., G. Ancellet, H. Bessafi, A. Badr, and D. Lan Sun Luk, Field observations of the vertical distribution of tropospheric ozone at the island of Reunion (southern tropics), *J. Geophys. Res.*, *101*, 23,835–23,849, 1996.

Brasseur, G. P., D. A. Hauglustaine, S. Walters, P. J. Rasch, J.-F. Müller, C. Granier, and X. X. Tie, MOZART, A global chemical transport model for ozone and related chemical tracers: 1. Model description, *J. Geophys. Res.*, *103*, 28,265–28,289, 1998.

Chameides, W. L., D. D. Davis, G. L. Gregory, G. Sachse, and A. L. Torres, Ozone precursors and ozone photochemistry over eastern North Pacific during the spring of 1984 based on the NASA GTE/CITE 1 airborne observations, *J. Geophys. Res.*, *94*, 9799–9808, 1989.

Chatfield, R. B., Z. Guo, G. W. Sachse, D. R. Blake, and N. J. Blake, The subtropical global plume in the Pacific Exploratory Mission-Tropics A (PEM-Tropics A), PEM-Tropics B, and the Global Atmospheric Sampling Program (GASP): How tropical emissions affect the remote Pacific, *J. Geophys. Res.*, *107*(D16), 4278, doi:10.1029/2001JD000497, 2002.

Davis, D., J. Crawford, S. Liu, S. Mckeen, A. Bandy, D. Thornton, F. Rowland, and D. Blake, Potential impact of iodine on tropospheric levels of ozone and other critical oxidants, *J. Geophys. Res.*, *101*, 2135–2147, 1996.

de Laat, A. T. J., M. Zachariasse, G. J. Roelofs, P. van Velthoven, R. R. Dickerson, K. P. Rhoads, S. J. Oltmans, and J. Lelieveld, Tropospheric O_3 distribution over the Indian Ocean during spring 1995 evaluated with a chemistry-climate model, *J. Geophys. Res.*, *104*, 13,881–13,894, 1999.

Dickerson, R. R., K. P. Rhoads, T. P. Carsey, S. J. Oltmans, and P. J. Crutzen, Ozone in the remote boundary layer: A possible role for halogens, *J. Geophys. Res.*, *104*, 21,385–21,395, 1999.

Dulichand, K. S. Modh, M. Naja, S. Venkatramani, and S. Lal, Altitudinal trends in O_3, CO, CH_4 and SF_6 over the Indian Ocean during the INDOEX IFP-99 ship cruise, *Curr. Sci.*, *80*, 100–104, 2001.

Fishman, J. J., M. Hoell Jr., R. D. Bendura, R. J. McNeal, and V. W. J. H. Kirchoff, NASA GTE TRACE A Experiment (September–October 1992): Overview, *J. Geophys. Res.*, *101*, 23,865–23,879, 1996.

Hao, W. M., and M.-H. Liu, Spatial and temporal distribution of tropical biomass burning, *Global Biogeochem. Cycles*, *8*, 495–503, 1994.

Hauglustaine, D. A., G. P. Brasseur, S. Walters, P. Rasch, J. F. Müller, L. K. Emmons, and M. A. Carroll, MOZART, A global chemical transport model for ozone and related chemical tracers: 2. Model results and evaluation, *J. Geophys. Res.*, *103*, 28,291–28,335, 1998.

Holton, J. R., P. H. Haynes, M. E. McIntyre, A. R. Douglass, R. B. Rood, and L. Pfister, *Rev. Geophys.*, *33*(4), 403–439, 1995.

Horowitz, L. W., et al., A global simulation of tropospheric ozone and related tracers: Description and evaluation of MOZART, version 2, *J. Geophys. Res.*, *108*, doi:10.1029/2002JD002853, in press, 2003.

Intergovernmental Panel on Climate Change, *The Climate Change 2001: The Scientific Basis*, edited by J. T. Houghton et al., Cambridge Univ. Press, New York, 2001.

Kley, D., P. J. Crutzen, H. G. J. Smit, H. Voma, S. J. Oltmans, H. Grassl, and V. Ramanathan, Observations of near-zero ozone concentrations over the convective Pacific: Effects on air chemistry, *Science*, *274*, 230–233, 1996.

Lelieveld, J., et al., The Indian Ocean Experiment: Widespread air pollution from south and Southeast Asia, *Science*, *291*, 1031–1036, 2001.

McFiggans, G., J. M. C. Plane, B. J. Allan, L. J. Carpenter, H. Coe, and C. O'Dowd, A modeling study of iodine chemistry in the marine boundary layer, *J. Geophys. Res.*, *105*, 14,371–14,385, 2000.

Müller, J.-F., Geographical distribution and seasonal variation of surface emissions and deposition velocities of atmospheric trace gases, *J. Geophys. Res.*, *97*, 3787–3804, 1992.

Murphy, D. M., and D. W. Fahey, An estimate of the flux of stratospheric reactive nitrogen and ozone into the troposphere, *J. Geophys. Res.*, *99*, 5325–5332, 1994.

Olivier, J. G. J., and J. J. M. Berdowski, Global emissions sources and sinks, in *The Climate System*, edited by J. Berdowski, R. Guicherit, and B. J. Heij, pp. 33–78, A. A. Balkema, Brookfield, Vt., 2001.

Olivier, J. G. J., A. F. Bouwman, C. W. M. van der Maas, J. J. M. Berdowski, C. Veldt, J. P. J. Bloos, A. J. H. Visschedijk, P. Y. J. Zandveld, and J. L. Haverlag, Description of EDGAR version 2.0: A set of global emission inventories of greenhouse gases and ozone-depleting substances for all anthropogenic and most natural sources on a per country basis and on a 1 × 1 degree grid, *RIVM Rep. 77-1060-002*, Natl. Inst. of Public Health and the Environ., Bilthoven, Netherlands, 1996.

Peshin, S. K., T. K. Mandal, H. G. J. Smit, S. K. Srivastava, and A. P. Mitra, Observations of vertical distribution of tropospheric ozone over Indian Ocean and its comparison with continental profiles during INDOEX FFP-1998 and IFP-1999, *Curr. Sci.*, *80*, 197–208, 2001.

Prados, A. I., R. R. Dickerson, B. G. Doddridge, P. A. Milne, J. L. Moody, and J. T. Merrill, Transport of ozone and pollutants from North America to the North Atlantic Ocean during the 1996 Atmosphere/Ocean Chemistry Experiment (AEROCE) intensive, *J. Geophys. Res.*, *104*, 26,219–26,233, 1999.

Rhoads, K. P., P. Kelley, R. R. Dickerson, T. P. Carsey, M. Farmer, D. L. Davoie, and J. M. Prospero, Composition of the troposphere of the Indian Ocean during the monsoonal transition, *J. Geophys. Res.*, *102*, 18,981–18,995, 1997.

Roelofs, G. J., and J. Lelieveld, Model study of the influence of cross-tropopause O_3 transport on tropospheric O_3 levels, *Tellus, Ser. B*, *49*, 38–55, 1997.

Schultz, M. G., et al., On the origin of tropospheric ozone and NO_x over the tropical South Pacific, *J. Geophys. Res.*, *104*, 5829–5843, 1999.

Singh, H. B., et al., Low ozone in the marine boundary layer of the tropical Pacific Ocean: Photochemical loss, chlorine atoms, and entrainment, *J. Geophys. Res.*, *101*, 1907–1917, 1996.

Singh, H. B., et al., Biomass burning influences on the composition of the remote South Pacific troposphere: Analysis based on observations from PEM-Tropics A, *Atmos. Environ.*, *34*, 635–644, 2000.

Smit, H. G. J., et al., JOSIE: The 1996 WMO international intercomparison of ozonesonde under quasi flight conditions in the environmental simulation chamber at Jülich, in *Proceedings of XVIII Quadrennial Ozone Symposium*, edited by R. Bojkov and G. Visconti, pp. 971–974, Int. Ozone Comm., Int. Assoc. of Meteorol. and Atmos. Sci., Toronto, 1998.

Sreedharan, C. R., An Indian electrochemical ozonesonde, *J. Phys. E Sci. Instrum.*, *1*, 995–997, 1968.

Staudt, A. C., D. J. Jacob, J. A. Logan, D. Bachiochi, T. N. Krishnamurti, and N. Poisson, Global chemical model analysis of biomass burning and lightning influences over the South Pacific in austral spring, *J. Geophys. Res.*, *107*(D14), 4200, doi:10.1029/2000JD000296, 2002.

Stehr, J. W., W. P. Ball, R. R. Dickerson, B. G. Doddridge, C. A. Piety, and J. E. Johnson, Latitudinal gradients in O_3 and CO during INDOEX 1999, *J. Geophys. Res.*, *107*(D19), 8016, doi:10.1029/2001JD000446, 2002.

Vogt, R., P. J. Crutzen, and R. Sander, A mechanism for halogen release from sea-salt aerosol in the remote marine boundary layer, *Nature*, *383*, 327–329, 1996.

Weller, R., R. Lilischkis, O. Schrems, R. Neuber, and S. Wessel, Vertical ozone distribution in the marine atmosphere over the central Atlantic Ocean (56°S–50°N), *J. Geophys. Res.*, *101*, 1387–1389, 1996.

World Meteorological Organization, Third WMO inter-comparison of the ozonesonde used in the Global Ozone Observing System (Vanscoy, Canada 13–24 May, 1991), *Global Atmos. Watch Rep. 27*, Geneva, Switzerland, 1994.

Zachariasse, M., P. E. J. Van Veelthoven, H. G. J. Smit, J. Lelieveld, T. K. Mandal, and H. Kelder, Influence of stratosphere-troposphere exchange on tropospheric ozone over the tropical Indian Ocean during the winter monsoon, *J. Geophys. Res.*, *105*, 15,403–15,416, 2000.

―――――――――――
G. Beig (corresponding author) and N. Saraf, Indian Institute of Tropical Meteorology, PMA Division, Pashan, Dr. Homi Bhabha Road, Pune M.S. 411 008, India. (beig@tropmet.res.in; saraf_2000_in@yahoo.com)

M. G. Schultz, Max-Planck-Institut für Meteorologie, Bundesstraße 55, Hamburg 20146, Germany. (martin.schultz@dkrz.de)